A Breakdown Criterion of Free Molecular Flows and an Optimum Analysis of EBPVD

Shuai-Hui Li, Jing Fan, Yong-Hua Shu

Laboratory of High Temperature Gas Dynamics, Institute of Mechanics, Chinese Academy of Sciences, Beijing, China 100190

Abstract: Two important issues in electron beam physical vapor deposition (EBPVD) are addressed. The first issue is a validity condition of the classical cosine law widely used in the engineering context. This requires a breakdown criterion of the free molecular assumption on which the cosine law is established. Using the analytical solution of free molecular effusion flow, the number of collisions (N_c) for a particle moving from an evaporative source to a substrate is estimated that is proven inversely proportional to the local Knudsen number at the evaporation surface. $N_c = 1$ is adopted as a breakdown criterion of the free molecular assumption, and it is verified by experimental data and DSMC results. The second issue is how to realize the uniform distributions of thickness and component over a large-area thin film. Our analysis shows that at relatively low evaporation rates the goal is easy achieved through arranging the evaporative source positions properly and rotating the substrate.

Keywords: free molecular assumption, breakdown criterion, optimization, thin film, EBPVD.
PACS: 47.45. -n, 47.45. Dt, 82.45. Mp, 81.15. Jj.

INTRODUCTION

Electron beam physical vapor deposition (EBPVD) is an essential way to fabricate thin films. According to the classical cosine law [1], the particle flux on a substrate element A from an evaporation source may be written as

$$\frac{q_A}{q_s} = \frac{\delta A \cos\phi \cos\psi}{\pi r^2}, \tag{1}$$

where δA is the element area, r is the distance from element A to the center of an evaporation source O, and q_s is the evaporation rate.

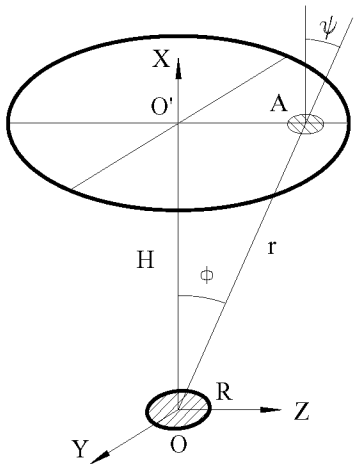

FIGURE 1. Schematic diagram of the cosine law with a circular evaporation source.

CP1084, *Rarefied Gas Dynamics: 26th International Symposium*, edited by T. Abe
© 2009 American Institute of Physics 978-0-7354-0615-5/09/$25.00

The cosine law (1) is widely used in the engineering context because it is simple and intuitive. As shown in Fig.1, the cosine law is based on the free molecular assumption. There were many studies on the continuum breakdown criteria [2-5], but few works has been carried out about a validity condition of the free molecular assumption. In the present paper, a breakdown criterion of the free molecular assumption is firstly derived. Then, the criterion is validated through comparing with experimental data and DSMC results. Next, our experimental facility of EBPVD is taken as an example to analyze how to realize the uniform distributions of thickness and component over a large-area thin film.

A BREAKDOWN CRITERION ON FREE MOLECULAR FLOWS

Consider a circular evaporation source of EBPVD. The origin of a rectangular coordinate system lies at the center of the circle O (Fig. 1).

The number of collisions for a particle moving along line OA is estimated as

$$N_c = \int_A^B \frac{dl}{\lambda(X,Z)} \approx \int_0^{H/\cos\phi} \frac{dl}{\lambda(X,Z)}, \tag{2}$$

where $\lambda(X,Z)$ is the local mean free path, and the approximation on the right-hand side of Eq. (2) is valid when the distance between an evaporation source and a substrate, H, is much larger than the former diameter D=2R.

It is known that the mean free path is inversely proportional to the number density for hard-sphere molecules, and therefore

$$\frac{\lambda_s}{\lambda(X,Z)} = \frac{n(X,Z)}{n_s}, \tag{3}$$

where the subscript s denotes the evaporation source. n_s and λ_s depend upon the evaporation rate Γ_s, and they are constant for a certain value of Γ_s.

The number density distributions for free molecular effusion flows with different exits in shape were generally considered by Cai [6], and the following expression was given for a circular exit with a zero average speed

$$\frac{n(X,Z)}{n_s} = \frac{1}{2} - \frac{X}{4\pi}\int_{-\pi}^{\pi} \frac{X^2+Z^2-ZR\sin\theta}{\left(X^2+Z^2\cos^2\theta\right)\sqrt{X^2+Z^2+R^2-2ZR\sin\theta}}\,d\theta. \tag{4}$$

We employ Eq. (4) to estimate the number density distribution in the vicinity of a free molecular regime. Substitution of Eqs. (3) and (4) into (2), we have

$$\begin{aligned} N_c &= \frac{1}{\lambda_s}\int_0^{H/\cos\phi}\left[\frac{1}{2} - \frac{X}{4\pi}\int_{-\pi}^{\pi} \frac{X^2+Z^2-ZR\sin\theta}{\left(X^2+Z^2\cos^2\theta\right)\sqrt{X^2+Z^2+R^2-2ZR\sin\theta}}\,d\theta\right]dl \\ &= \frac{1}{\lambda_s}\int_0^{H/\cos\phi}\left[\frac{1}{2} - \frac{l\cos\phi}{4\pi}\int_{-\pi}^{\pi} \frac{l^2-lR\sin\phi\sin\theta}{\left(l^2-l^2\sin^2\phi\sin^2\theta\right)\sqrt{l^2+R^2-2lR\sin\phi\sin\theta}}\,d\theta\right]dl \\ &= \frac{H}{2\lambda_s\cos\phi} - \frac{\cos\phi}{4\pi\lambda_s}\int_{-\pi}^{\pi}\frac{1}{\left(1-\sin^2\phi\sin^2\theta\right)}\int_0^{H/\cos\phi}\frac{l-R\sin\phi\sin\theta}{\sqrt{l^2+R^2-2lR\sin\phi\sin\theta}}\,dl\,d\theta \end{aligned} \tag{5}$$

When $\phi = 0$, the right-hand side of Eq. (5) can be exactly integrated. Neglecting the second order term of R/H, the expression is simplified as

$$N_c = \frac{H-\sqrt{H^2+R^2}+R}{2\lambda_s} \approx \frac{R}{2\lambda_s} = \frac{D}{4\lambda_s} = \frac{1}{4Kn_s}, \tag{6}$$

where $Kn_s = \lambda_s/D$ is the local Knudsen number at the evaporation source surface.

When $\phi \neq 0$, neglecting the second and high order terms of D/H, an approximate solution of the right-hand side of Eq. (5) is obtained as follows

$$N_c \cong \frac{1}{4\cos\phi Kn_s}. \tag{7}$$

Because ϕ is usually small in practice, $\cos\phi$ is of the order of unity.

According to Eq. (6) or (7), when $Kn_s > 0.5$, the number of collisions for an evaporative particle along its flight path is less than 0.5. It means that the effusion flow of the evaporation source satisfies the free molecular assumption, and the film thickness and component distributions follow the cosine law. $Kn_s = 0.25$ is adopted as a breakdown criterion on the free molecular assumption.

VALIDATION OF THE BREAKDOWN CRITERION

The criterion (6) is validated in comparison with experiments and DSMC calculations as follows. Our experimental facility of EBPVD [7] is shown in Fig. 2. It has a cylindrical vacuum chamber with a diameter of 760mm, a height of 850mm, and water cooled side-wall. Three sets of electron guns and evaporation crucibles G1-G3 are equipped inside the chamber. There are three quartz crystal probes P1-P3 used to monitor and control independently the evaporation rates of the corresponding sources. The wafer can rotate driven by a motor. A typical background pressure during a deposition process keeps about 10^{-3}Pa.

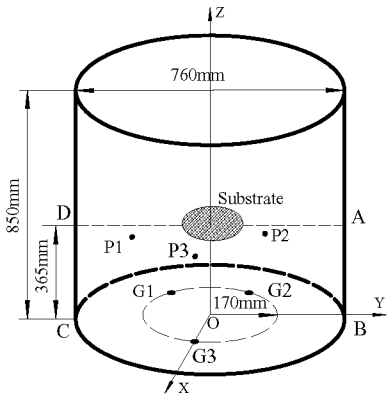

FIGURE 2. Schematic diagram of the positions of the evaporation sources (G1, G2, G3), quartz crystal probes, and substrate in our experimental facility of EBPVD.

As shown in Table 1, Case 1 considers yttrium and titanium co-evaporation using the sources G1 and G2. The deposition process lasts about 1000 seconds. The yttrium and titanium ingots are weighed with an electronic microbalance before and after the experiment. The evaporation rates $\Gamma_s = q_s / A_s$ are easily determined from the measured total evaporation masses and evaporation areas A_s and the deposition time, and an equivalent diameter of the evaporation source is defined as $D = \sqrt{4A_s/\pi}$ (Table 1).

The relation of Γ_s to an evaporation surface temperature T_s was provided by Dushman [8]

$$\log \Gamma_s = C - 0.5 \log T_s - B/T_s \,. \tag{8}$$

The fitting values of B and C for common metals may be found in Table 10.2 of Ref. [8], which are 2.197×10^4 and 9.17 for yttrium, and 2.323×10^4 and 9.11 for titanium, respectively.

It is known that Γ_s has the following form in the kinetic theory [9, 10]

$$\Gamma_s = \frac{1}{4} m n_s \bar{c}_s \,, \tag{9}$$

where $\bar{c}_s = \sqrt{8kT_s/\pi m}$.

TABLE 1. The values of Kn_s at different experimental and computational conditions.

Case	Sources	H (m)	D (cm)	Γ_s (10^{-3}kg/m^{2}s)	n_s (10^{19}/m^3)	λ_s (cm)	Kn_s	N_c
1	Yt	0.37	3.0	2.6	3.1	1.56	0.52	0.5
	Ti	0.37	1.2	2.1	12.6	0.39	0.33	0.8
2 [12]	Yt	0.38	3.4	10.0	38.3	0.13	0.04	6.6
3 [12]	Yt	0.38	3.4	0.8	2.9	1.67	0.50	0.5
4 [13]	Yt	0.38	3.4	7.6	28.6	0.17	0.05	5.0
	Ba	0.38	3.4	23.4	103.0	0.04	0.01	20.8
	Cu	0.38	3.4	16.4	80.9	0.05	0.02	15.6

Because the values of Γ_s are known in experiment, n_s can be numerically solved from Eqs. (8) and (9), they are also given in Table 1.

In Case 1, the origin of a 4-inch silicon wafer is located exactly above the midpoint of G1 and G2 (Fig. 2). The crystal symbol is close to G1, while the shield slices are parallel to the Y direction (Fig.3a). As shown in Fig. 3a, there are 18 positions for measuring the film thickness and the molar ratio after the experiment. Measurements are carried out in all these positions using a Rutherford backscattering spectrometer (RBS) that may obtain the thickness and molar ratio in the meantime, profilometer measurements are performed in 12 of them (except positions 3, 4, 9, 10, 15 and 16), another way to measure the molar ratio with an inductively coupled plasma atomic emission spectrometer (ICP-AES) is performed in four positions (1, 5, 8 and 17).

As shown in Figs. 3b) and 3c), the cosine law in general agrees well with the DSMC and experimental results. This is in accordance with our criterion because the values for yttrium and titanium are both larger than 0.5. Due to the page limitation, more details are not included here that can be found in Ref. [11].

According to our criterion, the cosine law does not work for Case 2 but is accurate for Case 3 because the values of Kn_s are 0.04 and 0.50, respectively (see Table 1). This is nicely verified by Fig. 13 and 8 of [12] where the collisionless deposition thickness profiles for Cases 2 and 3 were compared with the corresponding DSMC profiles and experimental data, respectively. A significant deviation was seen in the former, in contrast to an excellent agreement in latter.

A similar situation occurs in Case 4. The values of Kn_s for three sources with different evaporation materials are all larger than the critical value for the free molecular assumption to be valid. This is also verified by Fig. 6b) of [13] where the thickness and component profiles given by DSMC were far away from the cosine law.

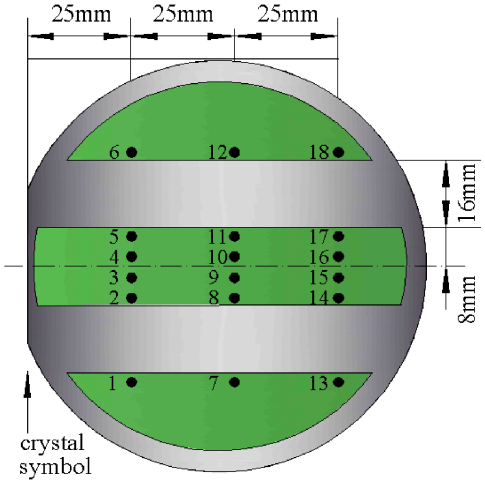

(a) Positions to measure the thickness and combining proportion of Yt-Ti alloy film over a 4-inch silicon wafer

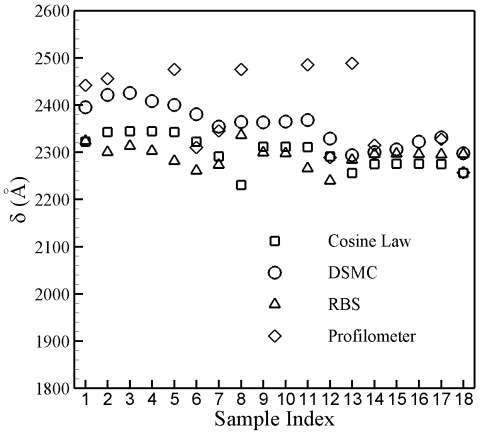

(b) Thickness

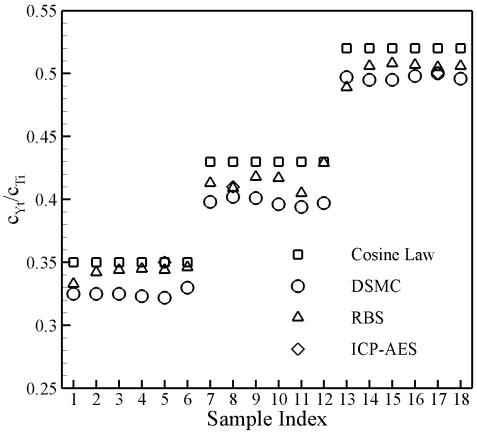

(c) Molar ratio of Yt to Ti

FIGURE 3. The thickness and component distributions of Yt-Ti alloy film over a 4-inch wafer for Case 1.

Fig. 4 compares the deposition thickness profiles of yttrium in situations similar to Cases 2 and 3 but with different values of Kn_s that is adjusted through the evaporation rates. The normalized factor $\delta_{\cos}$ is the thickness at the substrate center given by the cosine law. It is seen that the DSMC profiles agree well with the cosine law when $Kn_s \geq 1$. When Kn_s decreases to 0.1, the collision effect becomes important that makes the DSMC profile significantly different from the cosine law.

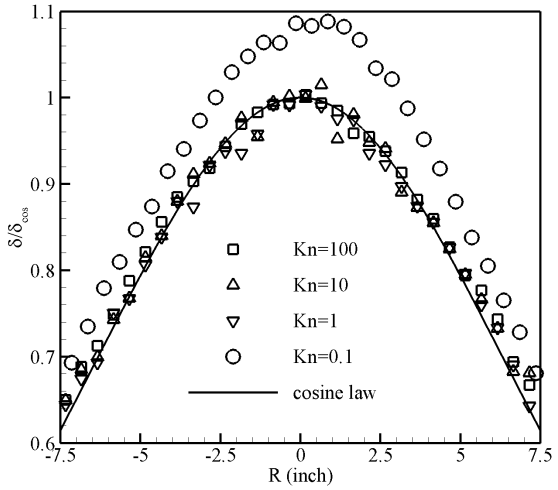

FIGURE 4. Comparison of normalized thickness profiles given by the cosine law and DSMC in situations similar to Cases 2 and 3 but with different Kn_s.

AN OPTIMUM ANALYSIS OF EBPVD

For low and even moderate evaporation rates with $Kn_s > 0.5$, the free molecular assumption is valid. Using the cosine law (1), the particle flux from an evaporation source in our experimental facility (Fig.3) may be expressed as

$$\frac{\overline{q}_{A,i}}{q_{s,i}} = \int_0^{\Delta t} \frac{\delta A \cos\phi \cos\psi}{\pi r^2} dt = \int_0^{\Delta t} \frac{\delta A H^2}{\pi r^4} dt$$
$$= \frac{\delta A H^2}{\pi} \int_0^{\Delta t} \frac{dt}{\left\{\left[R_A \cos(\theta_A + \omega t) - R_i \cos\theta_i\right]^2 + \left[\left(R_A \sin(\theta_A + \omega t) - R_i \sin\theta_i\right)\right]^2 + H^2\right\}^2} \tag{10}$$

where the over bar denotes averaging over a time interval, R_i is the distance of the center of evaporation source i from O, R_A is the distance of element A from a wafer center O' exactly above the origin O, θ_i and θ_A are the initial phase angles of the center of evaporation source i and element A, respectively, and ω is the rotation speed of the wafer around O'.

Let $\Delta t = 2\pi/\omega$, $\theta = \theta_A + \omega t$, and $\vartheta = \theta - \theta_i$, Eq. (10) may be transformed as

$$\frac{\overline{q}_{A,i}}{q_{s,i}} = \frac{\delta A H^2}{\pi} \int_0^{2\pi} \frac{d\theta}{\pi\left[\left(R_A \cos\theta - R_i \cos\theta_i\right)^2 + \left(R_A \sin\theta - R_i \sin\theta_i\right)^2 + H^2\right]^2}$$
$$= \frac{\delta A H^2}{\pi} \int_0^{2\pi} \frac{d\theta}{\left[R_A^2 + R_i^2 + H^2 - 2R_A R_i \cos(\theta - \theta_i)\right]^2} = \frac{2\delta A H^2}{\pi} \int_0^{\pi} \frac{d\vartheta}{\left[R_A^2 + R_i^2 + H^2 - 2R_A R_i \cos\vartheta\right]^2} \tag{11}$$

According to Eq. (11), if all evaporation sources regularly lie on a circle and a wafer rotates around the circle center at a constant speed, the molar ratio between any two deposition components over the whole wafer is the same as the ratio between the corresponding evaporation rates.

For our EBPVD facility, $H = 365mm$, $R_i = 170mm$, and $R_A \leq 76mm$. Substituting these values into Eq. (11), a numerical solution shows that the maximum thickness difference between the center and outer edge of the 6-inch wafer is about 3% only.

CONCLUDING REMARKS

Through estimating the number of collisions for a particle along its flight path, a breakdown criterion on the free molecular assumption was obtained. According to the criterion, when the local Knudsen number at the evaporation source surface is more than 0.5, the classical cosine law based on the free molecular assumption can be used to predict accurately the deposition thickness and component distributions in EBPVD.

For relatively low evaporation rates, optimum deposition conditions for large-area, multi-component films were carried out based on the cosine law. It was shown that when all the evaporation sources lie on the same circle and a wafer exactly above the circle rotated uniformly around its center, the molar ratio between any two deposition components over the whole wafer was the same.

ACKNOWLEDGEMENTS

This work is partially supported by the National Natural Science Foundation of China under Grant No. 90205024, 10502051 and 10621202.

REFERENCES

1 Holland L and Steckelmacher W. The Distribution of Thin Films Condensed on Surfaces by the Vacuum Evaporation Method. Vacuum, 1952, 2: 346-364.
2 Bird G A. Breakdown of Translational and Rotational Equilibrium in Gaseous Expansions. AIAA Journal, 1970, 8: 1998-2003.
3 Boyd I D and Chen G. Predicting Failure of the Continuum Fluid Equation in Transitional Hypersonic Flows. Phys. Fluids, 1995, 7: 210-219.
4 Wang W L and Boyd I D. Predicting Continuum Breakdown in Hypersonic Viscous Flows. Phys. Fluids, 2003, 15: 91-100.
5 Macrossan M N. Scaling Parameters for Hypersonic Flow: Correlation of Sphere Drag Data. Rarefied Gas Dynamics 25, edited by M.S. Ivanov & A.K. Rebrov, 2006, pp759-764..
6 Cai C P. Theoretical and Numerical Studies of Plume Floes in Vacuum Chambers. Ph.D Dissertation, the University of Michigan, 2005.
7 Fan J, Shu Y H, Liu H L and Li S H. Electron Beam Physical Vapor Deposition. IMCAS STR 2005003, Institute of Mechanics, Chinese Academy of Sciences, 2005. (in Chinese).
8 Dushman S. Scientific Foundation of Vacuum Technology, New York: John Wiley & Sons, 1962.
9 Bird G. A. Molecular Gas Dynamics and the Direct Simulated of Gas Flows, Clarendon Press, 1994.
10 Shen C. Rarefied Gas Dynamics: Fundamentals, Simulations and Micro Flows, Berlin: Springer, 2005.
11 Li S H, Shu Y H, Fan J. Thickness and Component Distributions of Yttrium-Titanium Alloy Films in Electron-Beam Physical Vapor Deposition. Science in China Series E, 2008, 51(9): 1470-1482.
12 Fan J, Boyd I D, Shelton C. Monte Carlo Modeling of Electron Beam Physical Vapor Deposition of Yttrium. J. Vac. Sci. Technol. A, 2000, 18: 2937-2945.
13 Fan J, Boyd I D, Shelton C. Monte Carlo Moldeling of YBCO Vapor Deposition. Rarefied Gas Dynamics 22, edited by T. J. Bartel and M. A. Gallis, 2000, pp214-221.